DOI: 10.1002/ejic.201000170

Reaction Medium pH Dependent Existence of Mn^{II} Bound [ON] Donor Zwitterionic Chelating Ligand and Self-Assembly of Hydroxido-Bridged Mn^{II}_4 Cluster

Mrinal Sarkar,[a] Valerio Bertolasi,[b] and Debashis Ray*[a]

Keywords: N,O ligands / Bridging ligands / Schiff bases / Manganese / Zwitterions

A mononuclear MnN_4O_2 complex with two zwitterionic ligands and a centrosymmetric tetranuclear μ_3-OH-bridged self-assembled Mn_4 cluster were synthesized and characterized by using the [NO(H)N] ligand H_{OPh}bip [2,6-bis(phenylmethyliminomethyl)-4-methylphenol]. The reaction in MeOH in the presence of NH_4SCN and a lower stoichiometry of $Mn(OAc)_2\cdot 4H_2O$ without any added base produces $[Mn^{II}(H_Nbip)_2(NCS)_2]\cdot CH_3CN$ (**1**$\cdot CH_3CN$). In the presence of NaOH and NH_4SCN in MeOH, the cluster $[Mn^{II}_4(\mu\text{-bip})_2(\mu_3\text{-OH})_2(NCS)_4]$ (**2**), featuring a stepped-cubane, was obtained through hydroxido-bridge-driven dimerization of two μ_3-OH-bridged $[Mn_2]$ fragments derived from **1**$\cdot CH_3CN$.

Introduction

Manganese is known to be present in the active sites of several metalloenzymes, such as manganese catalase, superoxide dismutase (SOD), extradiol dioxygenase, arginase, ribonucleotide reductase, the oxygen-evolving complex (OEC) of photosystem II (PS II), and lipoxygenase.[1] Both mononuclear and tetranuclear manganese complexes are of considerable interest as structural models following the identification of the mononuclear centers in oxalate decarboxylases (OxDC)[2] and oxalate oxidases (OxOx)[3] and Mn_4 assembly in PS II.[4] X-ray crystallographic studies have shown the presence of distorted octahedral Mn^{II} ions coordinated to three N atoms of histidine and one O atom of glutamate residues, and two O atoms of water molecules in the OxOx enzyme.[5] The coordination of water or its derivatives (HO^- or O^{2-}) in the formation of aggregates of transition-metal ions is of great significance. Many Mn_4 complexes containing hydroxido, oxido, and peroxido bridges have been synthesized and characterized, where the bridging potential of these coupling groups are utilized for dimerization and self-assembly.[6] Bridges like μ_3-O and μ_3-OMe are more frequently found.[7] However, only two μ_3-hydroxido-bridged tetranuclear manganese complexes that include $Mn^{II}Mn^{III}(\mu_3\text{-OH})$[8] and $Mn^{II}(\mu_3\text{-OH})$[6c] bonds are known. As of now, manganese-based small clusters, which act as single molecule magnets (SMMs),[9] are useful species for enhancing our understanding of SMM behavior. Creation of mononuclear manganese(II) and its self-assembled tetranuclear congener of the same ligand system is of great synthetic value in understanding the formation and growth of the different manganese active sites in biology and magnetic materials.

In this background we have focused our attention to the [NON] donor Schiff base ligand 2,6-bis(phenylmethyliminomethyl)-4-methylphenol (H_{OPh}bip, H_{OPh} is the proton attached to phenolate oxygen atom; Scheme 1).

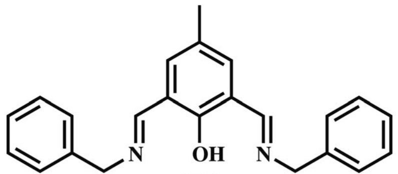

Hbip

Scheme 1.

In the neutral pH range (pH ≈ 7) and in the metal bound form it may exist as zwitterion $H_N$bip with nonadjacent positive and negative charges. This ampholyte form can function as a [NO] donor bidentate neutral ligand. At higher pH values, deprotonation of H_{OPh}bip affords the potentially binucleating bis-bidentate [NON] donor ligand bip^- possessing the potential to act in both chelating and bridging capacities. In this pH range, the availability of HO^- groups leads to zwitterionic proton abstraction, coordination, bridge, and self-condensation to a Mn_4 complex. The intention to use this type of ligand is to generate coordinatively unsaturated manganese sites, which is favored by the low denticity of the ligand. This could then simultaneously bind more than one thiocyanate anion through the forma-

---

[a] Department of Chemistry, Indian Institute of Technology,
Kharagpur 721302, India
Fax: +91-3222-82252
E-mail: dray@chem.iitkgp.ernet.in
[b] Dipartimento di Chimica e Centro di Strutturistica
Diffrattometica, Università di Ferrara,
via Borsari 46, 44100 Ferrara, Italy

Supporting information for this article is available on the WWW under http://dx.doi.org/10.1002/ejic.201000170.

tion of mononuclear and hydroxido-bridge-driven self-assembled clusters occupying the vacant positions in the coordination spheres.

The central phenolate group bearing a [NON] donor ligand in transition-metal assemblies is relatively new, although some notable results have been reported, consisting of a $[Zn_6]$[10] and a $[Cu_4]$ species.[11] Numerous Mn_4 clusters have been reported with the core structure varying from butterfly, cubane, double cubane, adamantane, square, basket, and linear to "pair-of-dimer", among many others.[6a,6b,9c,12] There have been many concepts and ideas to predict which species will self-assemble in solution, and these considerations are mainly based on the information stored in the coordinatively unsaturated dinuclear building units, their positioning in space, and metal-ion electronic configurations. Surprisingly, a Mn_4 cluster having a stepped-cubane core structure and different coordination geometries has not been reported, although the topology is rather simple. The tendency of manganese ions to accept a fifth ligand at the apical coordination site extends the bridging ability of HO^- group in a μ_3 fashion and is responsible for associating two dinuclear units to a stepped-cubane structure. The stepped-cubane geometry is unusual in manganese coordination chemistry due to its restriction in coordination geometry, but it is known in copper complexes as a consequence of the "plasticity" of the copper coordination spheres.[13]

Herein we have investigated the reaction medium pH dependent binding behavior of bip^- toward manganese(II) and isolated the complexes resulting from the zwitterionic form of the ligand at neutral pH and the hydroxido-bridge-driven aggregation at high pH values. Reported here are the stable mononuclear and tetranuclear Mn^{II} complexes of $H_{OPh}bip$ resulting from the tuning of the reaction medium pH and from varying the metal/ligand stoichiometry. These two compounds were isolated and crystallographically characterized. The aggregating ability of bip^-, together with the added HO^- in alkaline medium and its μ_3 binding properties, was exploited here in the preparation of **2**.

Results and Discussion

Synthesis and Reactivity

The Schiff base 4-methyl-2,6-bis(phenylmethyliminomethyl)phenol (Hbip) was prepared (Scheme S1, Supporting Information) by following a literature procedure,[14] and its reaction with manganese(II) salts was investigated under different reaction conditions (Scheme 2). We carried out the reaction of $Mn(OAc)_2\cdot 4H_2O$ with Hbip [designated as HOPhbip in Equation (1)] and NH_4SCN in MeOH and in the absence of any externally added base and obtained $[Mn^{II}(HNbip)_2(NCS)_2]$ (**1**) in 74% yield (Scheme 2), which shows that the formation of the zwitterion of HNbip, in the presence of AcO^- ions, prevents full utilization of its metal ion binding ability. However, no sign of formation of any Mn_2 product such as **4** (Scheme 2) was observed, perhaps because of the additional stability of **1**, which crystallizes as a bis-chelated mononuclear transition metal complex of any binucleating ligand assembled through H-bonding. A proposal for the formation of the Mn_2 complex comes from our endeavors reported recently on the cobalt(II) chemistry with this ligand.[15] The use of NaOH in MeOH in the above-mentioned reaction inhibits the formation of the ligand zwitterion and results in the formation of complex **2** in a 69% yield [Equation (2), Scheme 2]. Interestingly, the reaction of $\mathbf{1}\cdot CH_3CN$ with $Mn(OAc)_2\cdot 4H_2O$ and NH_4SCN in methanolic NaOH resulted in the quantitative transformation of $\mathbf{1}\cdot CH_3CN$ into **2** in a 63% yield [Equation (3)]. The formation of both complexes is consistent with elemental analysis and electrical conductivity data in CH_3CN.

$$2H_{OPh}bip + Mn(OAc)_2\cdot 4H_2O + 2NH_4SCN \rightarrow [Mn(H_Nbip)_2(NCS)_2] + 2NH_4OAc + 4H_2O \tag{1}$$

$$2H_{OPh}bip + 4Mn(OAc)_2\cdot 4H_2O + 4NH_4SCN + 4NaOH \rightarrow [Mn_4(\mu\text{-}bip)_2(\mu_3\text{-}OH)_2(NCS)_4] + 4NH_4OAc + 4NaOAc + 18H_2O \tag{2}$$

$$[Mn(H_Nbip)_2(NCS)_2] + 3Mn(OAc)_2\cdot 4H_2O + 4NaOH + 2NH_4SCN \rightarrow [Mn_4(\mu\text{-}bip)_2(\mu_3\text{-}OH)_2(NCS)_4] + 4NaOAc + 2NH_4OAc + 14H_2O \tag{3}$$

We failed to prepare **3** in the absence of NaOH by following an attempted procedure of Equation (2) with an excess amount of NH_4SCN and a stoichiometric amount of NEt_3 (Scheme 2). Use of an excess amount of NH_4SCN even up to a molar ratio of 6:1 with respect to the metal salt could not substitute the bridging HO^- groups by NCS^- in **2** and afforded **1**.

Spontaneous Dimerization Reaction for Self-Assembly

The direct reaction of Hbip with $Mn(OAc)_2\cdot 4H_2O$, NH_4SCN, and NaOH yielded **2**. The N,O chelation of one bip^- around two Mn^{II} followed by binding of one NCS^- to each metal ion and one hydroxido bridge yielded the electroneutral intermediate **I** (Scheme S2, Supporting Information). Interaction toward dimerization of two such species takes place through two *apical* Mn–O interactions from hydroxido bridges to produce intermediate **II**, which finally separates as **2** from the reaction mixture.

Formation of Mn_4 Stepped-Cubane by Uphill Transformation of Bis-thiocyanato-Coordinated 1

In the absence of any hydroxido bases and in the presence of a large excess of thiocyanate anions the only product obtained was mononuclear manganese(II) complex **1**, in which the zwitterionic binucleating ligands function as neutral bidentate N,O ligands. The protonated imine functions remain H-bonded to phenolate oxygen atoms. In MeOH and in the presence NaOH, **1** undergoes a self-assembly reaction [Equation (3), vide infra] with extra $Mn(OAc)_2\cdot 4H_2O$ and NH_4SCN to yield **2**, spontaneously and quantitatively.

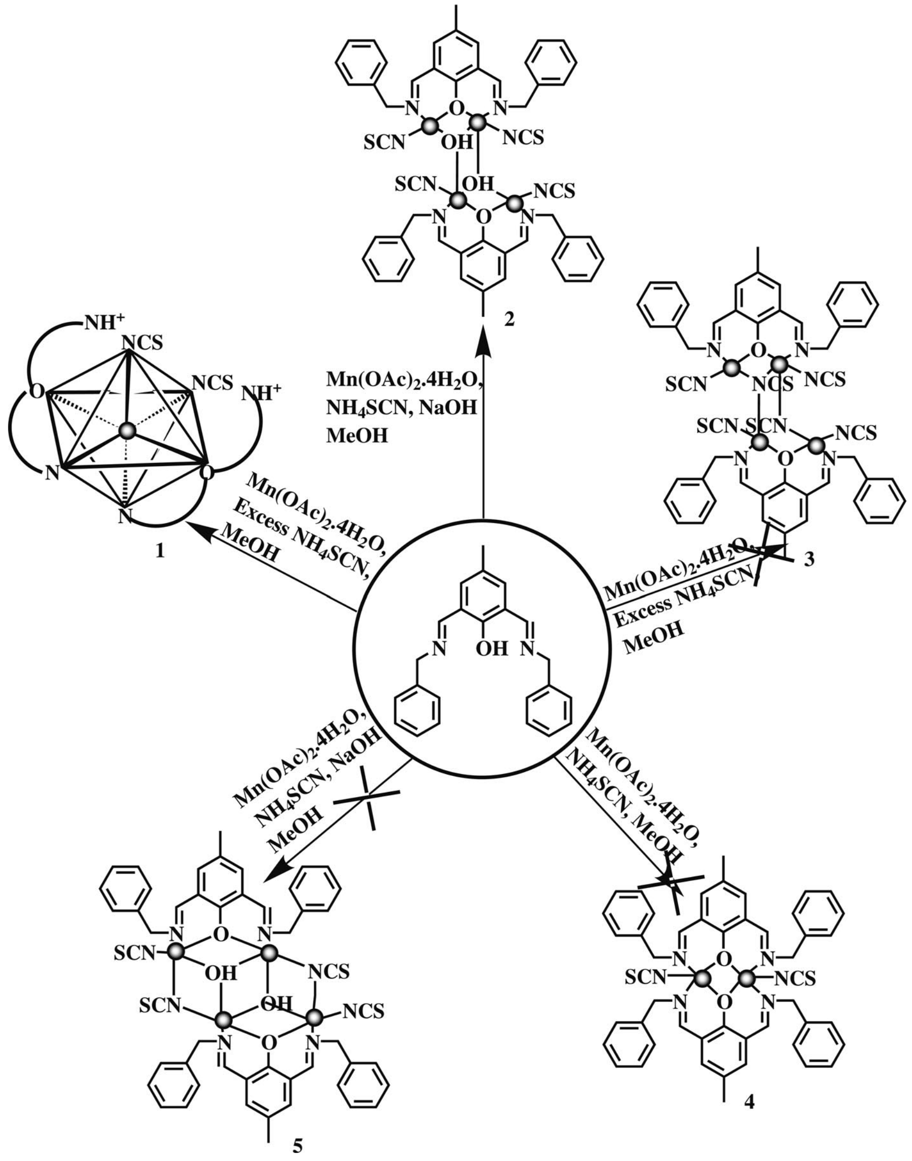

Scheme 2. Schematic representation of the ligand and thiocyanate assembly for Mn^{II} assembly against other unknown species.

FTIR Spectra

The sharp peak in the FTIR spectra of complexes **1** and **2** at 1647 and 1637 cm^{-1}, respectively, are characteristic of the C=N functionality of bip^{-}. For **2**, a broad and medium band at 3600 cm^{-1} is observed, which corresponds to the ν_{OH} stretching mode of the bridging HO^{-} groups.[16] The mode of binding of the thiocyanate anions in **1** and **2** was identified from the ν_{CN} stretching frequencies at 2060 and 2059 cm^{-1} for **1** and **2**, respectively, whereas the C–S stretching (ν_{CS}) and bending (δ_{NCS}) modes in the 700–825 cm^{-1} region could not be identified with certainty in the presence of strong absorptions by bip^{-} in this region.

Electronic Spectra

The d–d transition intensities of **1** and **2** are very low, as transitions from the $^6A_{1g}$ state to other higher states are doubly forbidden.[17] In MeCN solutions, the bands below 400 nm viz., at 215 (ε, 22680 $M^{-1}cm^{-1}$) and 260 nm (ε, 13970 $M^{-1}cm^{-1}$) for **1** and **2**, respectively, possibly originate from the $\pi \rightarrow \pi^*$ transition associated with the azomethine group.[18] Weak transitions at 410 (ε, 13170 $M^{-1}cm^{-1}$) and 450 nm (ε, 4780 $M^{-1}cm^{-1}$) for **1** and **2**, respectively, may be referred to the combination of metal-to-ligand charge transfer (MLCT) and d–d transitions.

Description of Structures

Single crystals suitable for X-ray structure determination were obtained by slow evaporation of a hot saturated CH_3CN solution of **1**·CH_3CN after 2 h and a CH_3CN/MeOH (1:1) solution of **2** after a week. Selected interatomic distances and angles are collected in Tables 1 and 2, and the crystallographic data are summarized in Table 3. The ORTEP diagrams of the two compounds are shown in Figures 1 and 2.

Table 1. Selected interatomic distances [Å] and angles [°] for complex **1**·CH_3CN.

	Distances		
Mn1–O1	2.0959(15)	Mn1–N5	2.242(2)
Mn1–O2	2.1177(15)	Mn1–N3	2.3158(19)
Mn1–N6	2.218(2)	Mn1–N1	2.3218(19)
	Angles		
O1–Mn1–O2	174.40(6)	N6–Mn1–N3	165.87(8)
O1–Mn1–N6	100.28(8)	N5–Mn1–N3	85.84(8)
O2–Mn1–N6	85.26(8)	O1–Mn1–N1	81.03(6)
O1–Mn1–N5	82.92(7)	O2–Mn1–N1	98.83(6)
O2–Mn1–N5	97.66(7)	N6–Mn1–N1	83.94(8)
N6–Mn1–N5	93.81(9)	N5–Mn1–N1	163.11(7)
O1–Mn1–N3	93.70(7)	N3–Mn1–N1	100.38(7)
O2–Mn1–N3	80.80(6)	N3–Mn1–N1	100.38(7)

Table 2. Selected interatomic distances [Å] and angles [°] for complex **2**.[a]

	Distances		
Mn1–N3	1.909(11)	Mn2–O2	1.958(6)
Mn1–O2	1.925(6)	Mn2–N2	1.962(8)
Mn1–N1	1.933(8)	Mn2–O1	1.968(6)
Mn1–O1	1.956(6)	Mn2–O2*	2.451(7)
Mn1–Mn2	2.9970(16)	O2–Mn2*	2.451(7)
Mn2–N4	1.933(9)	O2–Mn2*	2.451(7)
	Angles		
N3–Mn1–O2	92.3(3)	N2–Mn2–O1	91.4(3)
N3–Mn1–N1	97.4(4)	N4–Mn2–O2*	87.4(4)
O2–Mn1–N1	166.9(3)	O2–Mn2–O2*	82.5(3)
N3–Mn1–O1	165.7(4)	N2–Mn2–O2*	100.6(3)
O2–Mn1–O1	79.6(3)	O1–Mn2–O2*	96.5(2)
N1–Mn1–O1	92.6(3)	N4–Mn2–Mn1	129.6(3)
N3–Mn1–Mn2	129.1(3)	O2–Mn2–Mn1	39.07(18)
O2–Mn1–Mn2	39.88(19)	N2–Mn2–Mn1	130.7(2)
N1–Mn1–Mn2	133.0(3)	O1–Mn2–Mn1	40.07(17)
O1–Mn1–Mn2	40.35(17)	O2*–Mn2-Mn1	94.70(15)
N4–Mn2–O2	92.0(3)	Mn1–O1–Mn2	99.6(3)
N4–Mn2–N2	97.9(3)	Mn1–O2–Mn2	101.1(3)
O2–Mn2–N2	169.7(3)	Mn1–O2–Mn2*	105.1(3)
N4–Mn2–O1	169.0(4)	Mn2–O2–Mn2	97.5(3)
O2–Mn2–O1	78.5(2)	Mn2–O2–Mn2*	97.5(3)

[a] Symmetry operation: * $-x + 1, -y + 1, -z + 1$.

$[Mn^{II}(H_Nbip)_2(NCS)_2]\cdot CH_3CN$ ($1\cdot CH_3CN$)

Complex **1** forms orange crystals belonging to the monoclinic crystal system, space group $P2_1/n$. The ORTEP[19] representation of complex **1** (Figure 1) shows a mononuclear Mn^{II} cation that is six-coordinate in a distorted octahedral geometry in $N^{im/th}{}_4O_2$ (im and th stand for imine and thiocyanate nitrogen atoms) environments (Figure S1, Supporting Information). In the basal plane, two phenolate oxygen atoms (O1: 2.096 Å and O2: 2.117 Å) are in a *trans* disposition, and one nitrogen atom of the imine group (N3: 2.316 Å) from the zwitterionic $H_N$bip ligand and one nitrogen atom of NCS^- (N6: 2.218 Å) are coordinated to the Mn^{II} ion. The apical positions are occupied by the atoms N1 (2.321 Å) and N5 (2.242 Å) from $H_N$bip and NCS^-, respectively. The angular distortions are also noticeable with *trans* and *cis* angles in the 163–174 and 81–100° ranges, respectively. The two terminal NCS^- groups are coordinated differently to Mn^{II}, as evidenced from the Mn–N–C angles (174.15 and 138.94°). The negatively charged NCS^- groups bind more strongly to the Mn^{II} center (av. 2.230 Å) than the neutral imine functionalities (av. 2.319 Å).[20] The potentially binucleating Hbip ligand functions as a zwitterionic $[N^{im},O]$ donor bidentate ligand in **1** and is responsible for the formation of the *ctc* (*cis–trans–cis* orientations of N^{im}, O^{Ph}, and N^{th} donor atoms) isomer exclusively (Scheme 3) most probably due to the steric bulk of the ligand, which alters the coordination environment around the metal ion, and intramolecular H-bonding stabilization within the molecule.

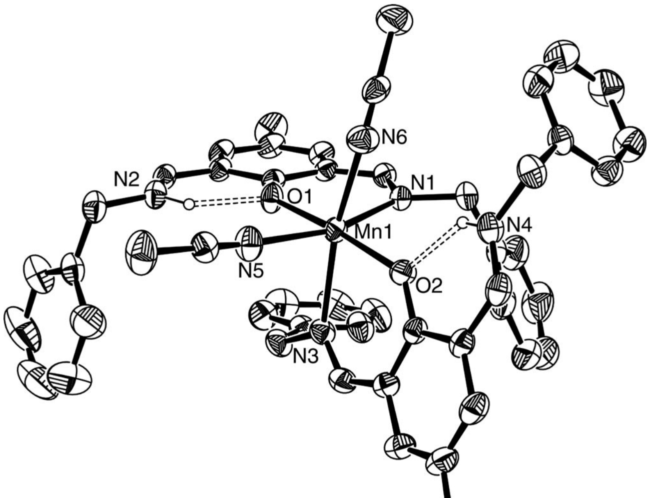

Figure 1. Labeled ORTEP view of $[Mn^{II}(NCS)_2(Hbip)_2]$; atom numbering scheme and thermal ellipsoids are drawn at the 30% probability level.

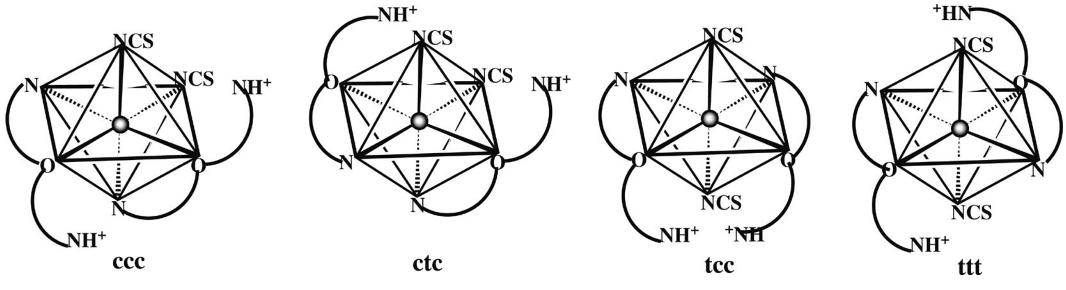

Scheme 3. Four possible isomers in the $N^{th}{}_2O_2N^{im}{}_2$ environment.

The noncoordinating imine groups of two ligands are protonated and H-bonded to the metal-bound phenolate oxygen atoms (N···O av. 2.572 Å, Figure 1). Compared to the distorted N_3O_3 coordination environments around the Mn^{II} ions in OxOx and OxDC, our complex has a N_4O_2 binding site. The average bond lengths around the Mn^{II} center observed in **1** (Mn–N$_{av}$: 2.274 Å, Mn–O$_{av.}$: 2.106 Å) are similar to those reported for the active site of OxDC (Mn–N$_{av.}$: 2.27 Å, Mn–O$_{carboxylate}$: 2.04 Å). This sort of mononuclear binding of any potential binucleating ligand is not reported in the literature. One representative diagram of the crystal packing along the *b* axis shows side-by-side placement of molecules (Figure S2, Supporting Information).

[Mn$^{II}_4$(μ-bip)$_2$(μ$_3$-OH)$_2$(NCS)$_4$] (2)

Complex **2** crystallizes as brown crystals that belong to the triclinic crystal system, space group $P\bar{1}$. The tetranuclear complex (Figure 2) can be described as [Mn$^{II}_2$(μ-bip)(μ-OH)(NCS)$_2$]$_2$ (Figure S3, Supporting Information), and it was obtained as a dimerized product of deprotonated bip$^-$ bound binuclear subunits. The Mn_4O_4 complex (O atoms are from PhO$^-$ and HO$^-$) is centrosymmetric with a central core of four Mn^{II} ions that can be described as a stepped-cubane (Figure S4, Supporting Information).[21] The stepped-cubane unit is a charge neutral aggregate of four Mn^{II} ions linked together by the template action of two HO$^-$ groups obtained from water molecules present in the solvent.

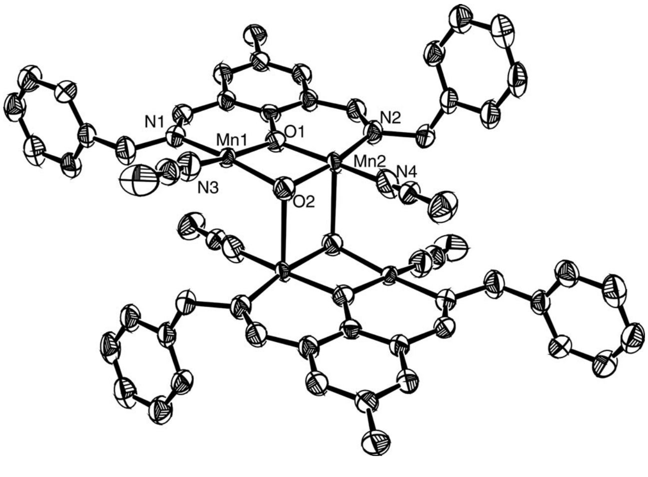

Figure 2. Labeled ORTEP view of [Mn$^{II}_4$(NCS)$_4$(μ$_3$-OH)$_2$(μ-bip)$_2$]; atom numbering scheme and thermal ellipsoids are drawn at the 30% probability level and H atoms are omitted for clarity.

Two imine nitrogen atoms of one ligand bound to two manganese and phenolate oxygen atom bridges to provide [Mn$^{II}_2$(μ-bip)(μ-OH)(NCS)$_2$] before the dimerization step. In the next step, two μ-OH$^-$ groups of two dimers expand their binding potential by making apical new bonds to two Mn^{II} ions. The structure can be described as two layers of dinuclear subunits linked by *basal* bridging of two phenolate O atoms (Mn–O av. 1.962 Å) of the ligand and two *apical* bridging by μ$_3$-OH$^-$ ions (Mn–O av. 2.446 Å; Figure S5, Supporting Information). The long *apical* Mn–OH bonds did not allow two SCN$^-$ terminals to establish bridging connectivity and octahedral coordinations to each manganese ion such as in **5** (Scheme 2). Thus, two four-coordinate square planar and two five-coordinate square pyramidal Mn^{II} centers in N_2O_2 and N_2O_3 coordination environments, respectively, are present within the stepped-cubane cluster having in-plane and out-of-plane av. Mn···Mn separations of 2.997 and 3.332 Å, respectively. The number of Mn_2O_2 rhombi present in complex **2** is three. Within the three Mn_2O_2 rhombi of the stepped-cubane structure, the av. Mn–O–Mn and O–Mn–O angles are 99.37 and 80.18°, respectively. Mn^{II} ions sit within perfect square planes (av. distance of Mn^{II} from the centroid of N_2O_2 squares are 0.011 and 0.059 Å) in SP–SPY (SP = square-planar; SPY = square-pyramidal) coordination geometries. The two terminal NCS$^-$ groups are coordinated differently to Mn^{II}, as evidenced from the Mn–N–C angles (172.91 and 157.44°). The bond lengths around the Mn^{II} centers observed in **2** (av. Mn–N^{im}: 1.947 Å, av. Mn–Nth: 1.920 Å, and av. Mn–O^{Ph}: 1.962 Å) are shorter than those observed in the case of **1** having wide variations (av. Mn–N^{im}: 2.319 Å, av. Mn–Nth: 2.230 Å, and av. Mn–O^{Ph}: 2.107 Å). The sum of the angles around the O atoms of the central phenolate and hydroxido bridges are 357.9 and 303.7°, respectively, which clearly demonstrates μ-planar and μ$_3$-pyramidal binding modes. Two sulfur ends of coordinated thiocyanate anions make complementary contacts with coordinated phenolate oxygen atoms with adjacent Mn_4 units (av. S···O 3.315 Å) and lead to a 1D network (Figure S6, Supporting Information).[22]

Cyclic Voltammetry

The redox behaviors of **1** and **2** were investigated by cyclic voltammetry in acetonitrile, under a nitrogen atmosphere at room temperature, in the potential range from +1.75 to –1.0 V vs. Ag/AgNO$_3$ at a scan rate of 100 mV s^{-1}. The data were recorded without stirring during the voltage sweeps and by using only freshly prepared solutions. A glassy-carbon working electrode and a Pt wire auxiliary electrode together with a 0.1 M solution of tetrabutylammonium perchlorate (TBAP) as supporting electrolyte were used. The voltammogram for complex **1**·CH$_3$CN is shown in Figure 3, and the data for compound **2** is provided in the Supporting Information.

Complex **1** shows one quasireversible process at $E_{1/2}$ = 1.1 V (ΔE_p = 0.27 V) attributed to the Mn^{II} → Mn^{III} process in the mononuclear species. In both OxDC and OxOx for oxidative oxalate metabolism, the Mn^{II} ion in the distorted octahedral N_3O_3 coordination domain acts as the catalytic center in the resting state. The catalysis is suggested to require a Mn^{II} → Mn^{III} oxidation process, where Mn^{III} is assumed to be the active oxidation level. Complex **2** displays two quasireversible processes at $E^1_{1/2}$ = 0.93 V (ΔE_p = 0.12 V) and $E^2_{1/2}$ = 1.23 V (ΔE_p = 0.14 V) and an

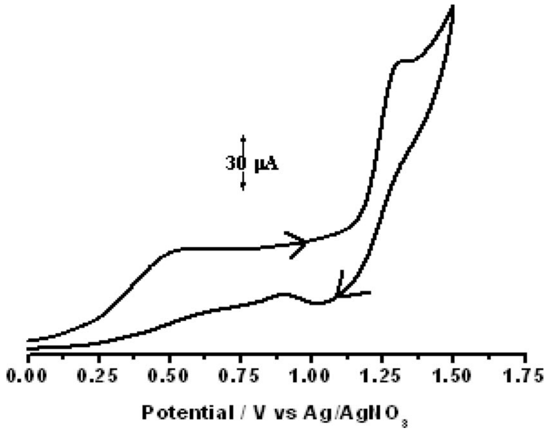

Figure 3. Cyclic voltammogram (scan rate 100 mV s^{-1}) of 10^{-3} M solutions of **1**·CH_3CN in CH_3CN at a glassy-carbon electrode (T = 293 K).

irreversible anodic peak at E_{pa} = 0.54 V (Figure S7, Supporting Information). The first response $E^1_{1/2}$ can be tentatively attributed to the Mn^{II} → Mn^{III} processes in the Mn_4 complex.[23]

Concluding Remarks

In summary, we have synthesized and characterized one mononuclear and one tetranuclear complex of manganese(II) with zwitterionic and anionic forms of a binucleating [NON] donor ligand. We also demonstrated the hydroxido-bridge-driven self-assembly and the transformation of **1**·CH_3CN into **2**. Supply of HO^- ions to the former deprotonates the iminium nitrogen atom of the zwitterionic ligand and allowed bridging of the two dinuclear units by two HO^- ions, which are found in the unsupported μ_3 coordination mode, leading to the formation of the $[Mn^{II}_4]$ complex. The conversion of **1**·CH_3CN into **2** also points to the role of HO^- ions in the formation of Mn_4 clusters in presence of extra metal ions and terminal thiocyanate ligands. We are currently working to exploit the asymmetry induced by external bridges in this reaction system to induce the formation of heterometallic high nuclearity assemblies.

Experimental Section

Materials: Sodium hydroxide, ammonium thiocyanate, and manganese acetate tetrahydrate were obtained from S. D. Fine Chem. (India), and benzylamine was obtained from SRL (India). All other chemicals and solvents were reagent-grade materials and were used as received without further purification.

Hbip Ligand: The Schiff base was prepared from the single-step condensation of 2,6-diformyl-4-methylphenol (1.640 g, 10 mmol) and benzylamine (2.18 mL, 20 mmol) in methanol (40 mL) under reflux for 1 h, as reported previously.[14]

$[Mn^{II}(H_Nbip)_2(NCS)_2]$·$CH_3CN$ (1·CH_3CN): To a yellow solution of Hbip (0.342 g, 1.00 mmol) in methanol (15 mL) was added a solution of $Mn(OAc)_2$·$4H_2O$ (0.122 g, 0.5 mmol) in methanol (20 mL). To the resulting orange-colored solution was dropwise added a solution of NH_4SCN (0.076 g, 1.00 mmol) in methanol (20 mL) with stirring at ambient temperature in air, and the reaction mixture was stirred for 1 h more, at which point it was deep orange in color. After evaporation of the reaction mixture an orange solid was obtained. The solid was isolated, washed with cold methanol, and dried under vacuum with P_4O_{10}. Orange single crystals suitable for X-ray analysis were obtained from hot MeCN over 2 h. Yield: 0.316 g (74 %). $C_{50}H_{47}MnN_7O_2S_2$ (897.03): calcd. C 66.94, H 5.28, N 10.93; found C 66.86, H 5.18, N 10.68. FTIR (KBr): $\tilde{\nu}$ = 3435 (br.), 2060 (vs), 1647 (vs), 1540 (vs), 1213 (m), 827 (m), 820 (m), 751 (m), 699 (m), 486 (m) cm^{-1}. Molar conductance (CH_3CN): Λ_M = 3.0 Ω^{-1} cm^2 mol^{-1}. UV/Vis (CH_3CN): λ (ε, M^{-1} cm^{-1}) = 410 (13170), 215 (22680) nm.

$[Mn^{II}_4(\mu\text{-bip})_2(\mu_3\text{-OH})_2(NCS)_4]$ (2)

Method A – Direct Route: To a yellow solution of Hbip (0.342 g, 1.00 mmol) in methanol (15 mL) was added a solution of $Mn(OAc)_2$·$4H_2O$ (0.490 g, 2.00 mmol) in methanol (20 mL). To the resulting orange-colored solution was dropwise added a solution of NH_4SCN (0.152 g, 2.00 mmol) in methanol (20 mL) with stirring at ambient temperature in air, and the reaction mixture turned deep orange in color. After 15 min, a solution of NaOH (0.080 g, 2.00 mmol) in methanol (15 mL) was added to the deep-orange-colored solution, and the reaction mixture was further stirred for 1 h. The deep-orange solution formed initially changed to brown in about 5 min. After evaporation of the reaction mixture a brown solid was obtained. The solid was isolated, washed with cold methanol, and dried under vacuum with P_4O_{10}. Brown single crystals suitable for X-ray analysis were obtained from MeCN over 7 d. Yield: 0.403 g (69 %). $C_{50}H_{44}Mn_4N_8O_4S_4$ (1168.96): calcd. C 51.37, H 3.79, N 9.58; found C 51.29, H 3.68, N 9.32. FTIR (KBr): $\tilde{\nu}$ = 3432 (br.), 2059 (vs), 1637 (vs), 1542 (vs), 1449 (m), 1217 (m), 1027 (br.), 827 (m), 753 (m), 700 (m), 601 (m), 486 (m) cm^{-1}. Molar conductance (CH_3CN): Λ_M = 6 Ω^{-1} cm^2 mol^{-1}. UV/Vis (CH_3CN): λ (ε, M^{-1} cm^{-1}) = 450 (4780), 260 (13970), 200 (21870) nm.

Method B – Uphill Transformation from 1: To an orange solution of **1**·CH_3CN (0.224 g, 0.25 mmol) in CH_3CN/MeOH (1:1, 30 mL) was added a solution of $Mn(OAc)_2$·$4H_2O$ (0.183 g, 0.75 mmol) in methanol (10 mL) followed by the dropwise addition of a solution of NH_4SCN (0.04 g, 0.50 mmol) in methanol (10 mL) with stirring at ambient temperature in air, and the reaction mixture turned deep orange in color. After 15 min, a solution of NaOH (0.04 g, 1.00 mmol) in methanol (10 mL) was added to the deep-orange-colored solution, and the reaction mixture was further stirred for 1 h. The deep-orange solution formed initially changed to brown in about 5 min. After evaporation of the reaction mixture a brown solid was obtained. The solid was isolated, washed with cold methanol, and dried under vacuum with P_4O_{10}. Yield: 0.184 g (63 %).

Physical Measurements: The elemental analyses (C, H, N) were performed with a Perkin–Elmer model 240C elemental analyzer. FTIR spectra were recorded with a Perkin–Elmer 883 spectrometer. The solution electrical conductivity and electronic spectra were obtained by using a Unitech type U131C digital conductivity meter with a solute concentration of about 10^{-3} M and a Shimadzu UV 3100 UV/Vis/NIR spectrophotometer, respectively.

Crystal Data Collection and Refinement for 1·CH_3CN and 2: The intensity data of complex **1**·CH_3CN was collected with a Bruker-APEX-2 CCD X-ray diffractometer by using graphite-monochromated Mo-K_α radiation (λ = 0.71073 Å) by the hemisphere method. The intensity data of complex **2** was collected with a Nonius CAD4 X-ray diffractometer by using graphite-monochromated Mo-K_α radiation (λ = 0.71073 Å) by the ω-scan method. Data were collected at 293 K. Information concerning X-ray data collection and structure refinement of the compound is summarized in Table 3. In the final cycles of full-matrix least-squares on F^2 all non-hydrogen atoms were assigned anisotropic thermal parameters. The positions of the H atoms bonded to C atoms were added (C–H distance 0.97 Å) in a riding model. The structure was solved by using the SHELX-97[24] program system. CCDC-697276 (for **1**·CH_3CN) and -697283 (for **2**) contain the supplementary crystallographic data for this paper. These data can be obtained free of charge from The Cambridge Crystallographic Data Centre via www.ccdc.cam.ac.uk/data_request/cif.

Table 3. Crystallographic data for **1**·CH_3CN and **2**.

	1·CH_3CN	**2**
Formula	$C_{50}H_{47}N_7O_2S_2Mn$	$C_{50}H_{44}N_8O_4S_4Mn_4$
M	897.03	1168.96
Space group	$P2_1/n$	$P\bar{1}$
Crystal system	monoclinic	triclinic
a [Å]	16.8499(7)	9.135(8)
b [Å]	13.6412(5)	11.687(3)
c [Å]	20.6317(8)	13.312(5)
α [°]	90	64.39(10)
β [°]	91.4090(10)	78.57(3)
γ [°]	90	77.32(3)
V [Å^3]	4740.8(3)	1241.7(5)
T [K]	293	293
Z	4	1
$D_{\text{calcd.}}$ [g cm^{-3}]	1.257	1.561
$F(000)$	1876	594
μ(Mo-K_α) [cm^{-1}]	4.13	12.16
Measured reflns.	63468	4362
Unique reflns.	10898	4362
R_{int}	0.0559	0.0000
Obs. reflns. $I \geq 2\sigma(I)$	6421	2418
$\theta_{\min}/\theta_{\max}$ [°]	1.54/27.62	1.71/24.97
Ranges h, k, l	–21/21, –16/17, –24/26	0/10, –13/13, –15/15
$R(F^2)$ (obs. reflns.)	0.0472	0.0728
$wR(F^2)$ (all reflns.)	0.1346	0.2359
No. variables	570	316
Goodness of fit	1.018	1.074
$\Delta\rho_{\max}$; $\Delta\rho_{\min}$ [e Å^{-3}]	0.341; –0.298	0.985; –0.682

Supporting Information (see footnote on the first page of this article): Synthesis of Hbip; proposed steps of aggregation of two [Mn^{II}_2] fragments in **2**; molecular structure of **1**·CH_3CN; packing diagram of complex **1**·CH_3CN; ORTEP view of the dinuclear segment present in [$Mn^{II}_4(NCS)_4(\mu_3\text{-}OH)_2(\mu\text{-bip})_2$]; molecular structure of **2**; stepped-cubane core view of **2**; intermolecular S···O contacts in **2** between phenolate oxygen and sulfur ends of thiocyanate anions; cyclic voltammogram of **2**.

Acknowledgments

M. S. is thankful to the Council of Scientific and Industrial Research, New Delhi for financial support. V. B. acknowledges the Italian Ministry of University and Scientific Research (MIUR), Rome.

[1] J. Reedijk, E. Bouwman, *Bioinorganic Catalysis*, Marcel Dekker Inc., New York, **1999**.

[2] A. Tanner, L. Bowater, S. A. Fairhurst, S. Bornemann, *J. Biol. Chem.* **2001**, *276*, 43627–43634.

[3] a) L. Requena, S. Bornemann, *Biochem. J.* **1999**, *343*, 185–190; b) C. H. Chang, D. Svedruić, A. Ozarowski, L. Walker, G. Yeagle, R. D. Britt, A. Angerhofer, N. G. J. Richards, *J. Biol. Chem.* **2004**, *279*, 52840–52849.

[4] L. V. Kulik, B. Epel, W. Lubitz, J. Messinger, *J. Am. Chem. Soc.* **2007**, *129*, 13421–13435.

[5] M. Scarpellini, J. Gätjens, O. J. Martin, J. W. Kampf, S. E. Sherman, V. L. Pecoraro, *Inorg. Chem.* **2008**, *47*, 3584–3593.

[6] a) S. Mukhopadhyay, R. J. Staples, W. H. Armstrong, *Chem. Commun.* **2002**, 864–865; b) R. Bagai, K. A. Abboud, G. Christou, *Dalton Trans.* **2006**, 3306–3312; c) L. Stelzig, B. Donnadieu, J.-P. Tuchagues, *Angew. Chem. Int. Ed. Engl.* **1997**, *36*, 2221–2222.

[7] a) T. Taguchi, M. R. Daniels, K. A. Abboud, G. Christou, *Inorg. Chem.* **2009**, *48*, 9325–9335; b) A. Igashira-Kamiyama, T. Kajiwara, M. Nakano, T. Konno, T. Ito, *Inorg. Chem.* **2009**, *48*, 11388–11393.

[8] Y. Sunatsuki, H. Shimada, T. Matsuo, M. Nakamura, F. Kai, N. Matsumoto, N. Re, *Inorg. Chem.* **1998**, *37*, 5566–5574.

[9] a) L. F. Jones, A. Prescimone, M. Evangelisti, E. K. Brechin, *Chem. Commun.* **2009**, 2023–2025; b) T. C. Stamatatos, K. A. Abboud, W. Wernsdorfer, G. Christou, *Inorg. Chem.* **2009**, *48*, 807–809; c) L. Lecren, O. Roubeau, Y.-G. Li, X. F. L. Goff, H. Miyasaka, F. Richard, W. Wernsdorfer, C. Coulon, R. Clérac, *Dalton Trans.* **2008**, 755–766.

[10] P. Roy, K. Dhara, M. Manassero, J. Ratha, P. Banerjee, *Inorg. Chem.* **2007**, *46*, 6405–6412.

[11] P. Roy, K. Dhara, M. Manassero, P. Banerjee, *Inorg. Chem. Commun.* **2008**, *11*, 265–269.

[12] a) C. J. Milios, A. Prescimone, A. Mishra, S. Parsons, W. Wernsdorfer, G. Christou, S. P. Perlepesd, E. K. Brechin, *Chem. Commun.* **2007**, 153–155; b) C. E. Dubé, D. W. Wright, S. Pal, P. J. Bonitatebus Jr., W. H. Armstrong, *J. Am. Chem. Soc.* **1998**, *120*, 3704–3716; c) M. K. Chan, W. H. Armstrong, *J. Am. Chem. Soc.* **1991**, *113*, 5055–5057; d) H. Chen, J. W. Faller, R. H. Crabtree, G. W. Brudvig, *J. Am. Chem. Soc.* **2004**, *126*, 7345–7349.

[13] a) L. Gazo, I. B. Bersuker, J. Garaj, M. Kabesova, J. Kohout, H. Langfeldorova, M. Serator, M. Melnik, F. Valach, *Coord. Chem. Rev.* **1976**, *19*, 253–297; b) N. J. Ray, L. Hulett, R. Sheahan, B. J. Hathaway, *J. Chem. Soc., Dalton Trans.* **1981**, 1463–1469.

[14] J. J. Grzybowski, F. L. Urbach, *Inorg. Chem.* **1980**, *19*, 2604–2608.

[15] M. Sarkar, R. Clérac, C. Mathonière, N. G. R. Hearns, V. Bertolasi, D. Ray, *Eur. J. Inorg. Chem.* **2009**, 4675–4685.

[16] H. Komatsuzaki, S. Ichikawa, S. Hikichi, M. Akita, Y. Morooka, *Inorg. Chem.* **1998**, *37*, 3652–3656.

[17] J. A. Hoshiko, G. Wang, J. W. Ziller, G. T. Yee, A. F. Heyduk, *Dalton Trans.* **2008**, 5712–5714.

[18] R. Cini, *Acta Crystallogr., Sect. C* **2001**, *57*, 1171–1173.

[19] M. N. Burnett, C. K. Johnson, *ORTEP III*, Report ORNL-6895, Oak Ridge National Laboratory, Oak Ridge, TN, **1996**.

[20] G. Das, R. Shukla, S. Mandal, R. Singh, P. K. Bharadwaj, *Inorg. Chem.* **1997**, *36*, 323–329.

[21] K. Isele, P. Franz, C. Ambrus, G. Bernardinelli, S. Decurtins, A. F. Williams, *Inorg. Chem.* **2005**, *44*, 3896–3906.

[22] C. Réthoré, A. Madalan, M. Fourmigué, E. Canadell, E. B. Lopes, M. Almeida, R. Clérac, N. Avarvari, *New J. Chem.* **2007**, *31*, 1468–1483.

[23] a) L. A. Reinhardt, D. Svedruzic, C. H. Chang, W. W. Cleland, N. G. J. Richards, *J. Am. Chem. Soc.* **2003**, *125*, 1244–1252; b) R. Anand, P. C. Dorrestein, C. Kinsland, T. P. Begley, S. E. Ealick, *Biochemistry* **2002**, *41*, 7659–7669.

[24] G. M. Sheldrick, *SHELX-97, Program for Crystal Structure Refinement*, University of Gottingen, Germany, **1997**.

Received: February 11, 2010